

# Time-Resolved Infrared Spectroscopic Studies of Poly(ethylene terephthalate) Deformation

Christian Pellerin,<sup>\*,†</sup> Michel Pérolet,<sup>‡</sup> and Peter R. Griffiths<sup>§</sup>

Département de chimie, Université de Montréal, Montréal, QC, H3C 3J7, Canada; Département de chimie, Université Laval, Québec, QC, G1K 7P4, Canada; and Department of Chemistry, University of Idaho, Moscow, Idaho 83844-2343

Received May 9, 2006; Revised Manuscript Received July 18, 2006

**ABSTRACT:** Polarization modulation infrared linear dichroism (PM-IRLD) and ultrarapid-scanning Fourier transform infrared spectroscopy (URS-FTIR) have been used to characterize the evolution of molecular orientation and microstructure during and following the step deformation of amorphous poly(ethylene terephthalate) (PET) above and below its glass transition temperature. The combined use of these techniques allowed a high sensitivity and an unprecedented 10 ms time resolution for the characterization of irreversible polymer deformation using infrared spectroscopy. PM-IRLD results show that the 1410  $\text{cm}^{-1}$  band of PET, often used as a thickness standard, presents a significant dichroism even at low draw ratios. Using this band, the relaxation kinetics of the phenyl ring was directly shown, for the first time, to be similar to that of the glycol group in amorphous PET. These results suggest that the relaxation proceeds mainly via cooperative motions involving at least one repeat unit and not only through rotations around the flexible  $\text{CH}_2\text{--CH}_2$  and  $\text{CH}_2\text{--O}$  bonds. The real-time study of the cold drawing of glassy amorphous PET by URS-FTIR showed that a large gauche-to-trans conversion (from ~15% to 60% of trans conformers) of the glycol groups occurs during the neck propagation. These trans conformers possess a very large and stable molecular orientation. Nevertheless, spectral analysis revealed that the “mesomorphic” phase, rather than the truly (all-trans) crystalline structure, is produced during cold drawing of PET at room temperature.

## Introduction

Infrared spectroscopy is widely used to characterize the structure–properties relationships in natural and synthetic polymers.<sup>1</sup> One of the most important structural parameters controlling the macroscopic properties of materials, such as spider silk and high-modulus polymeric fibers, is their degree of molecular orientation. Conventional infrared linear dichroism (IRLD) has been used for many years to probe the static molecular orientation in samples quenched below their glass transition temperature ( $T_g$ ) or in situ during slow deformations.<sup>2–5</sup> The main advantage of IRLD over other characterization techniques, such as birefringence and wide-angle X-ray diffraction, is that it can often be used to probe the orientation of multiple species or phases simultaneously. Indeed, its use has often revealed distinct orientation behavior for the different components and phases in semicrystalline polymers, polymer blends, and block copolymers, thus enabling a better understanding of their properties.<sup>3,4</sup>

Recently, more attention has been paid toward the real-time determination of orientation during rapid deformations and the direct determination of the relaxation kinetics following stretching. With a time resolution of the order of several seconds, conventional IRLD is too slow to perform such time-resolved experiments at deformation and relaxation rates relevant to processes such as industrial film blowing or spider silk spinning. However, technical developments in the past few years have significantly improved the time resolution of infrared spectroscopy for orientation characterization. In particular, polarization

modulation infrared linear dichroism (PM-IRLD)<sup>4,6</sup> and ultrarapid-scanning Fourier transform infrared spectroscopy (URS-FTIR)<sup>1,7</sup> have significantly enhanced the sensitivity and time resolution of infrared spectroscopy for the study of molecular orientation.

PM-IRLD uses a photoelastic modulator to rotate the polarization plane of the infrared radiation from parallel (p) to perpendicular (s) to the draw direction at a frequency of ~100 kHz. Using dual-channel acquisition electronics, this technique allows the direct measurement of the dichroic difference, thus allowing a much improved sensitivity as compared to conventional IRLD,<sup>8,9</sup> in addition to a time resolution as good as 400 ms.<sup>10,11</sup> URS-FTIR is a recently developed technique that uses a wedged rotating disk mirror to introduce the optical path difference in the interferometer.<sup>1,7,12</sup> Because there is no need to accelerate and decelerate a reciprocating moving mirror, this technique allows a greatly enhanced duty cycle and time resolution as compared to conventional FTIR spectrometers. Indeed, a time resolution of 5 ms per spectrum has been recently demonstrated for gas adsorption studies.<sup>13</sup>

In this work, we have used both PM-IRLD and URS-FTIR to study the evolution of molecular orientation and microstructure during and following the irreversible deformation of thin films of amorphous poly(ethylene terephthalate) (PET), a ubiquitous engineering polymer. The possibilities and limitations of these techniques for such studies will be contrasted.

## Experimental Section

PET films of 7  $\mu\text{m}$  thickness were prepared by blow molding and generously provided by Dr. K. C. Cole of the Industrial Materials Institute of the National Research Council of Canada. Differential scanning calorimetry characterization indicated that the samples were amorphous. Strips of 20 mm  $\times$  6 mm were deformed at room temperature and at 90 °C using a custom-built mechanical

<sup>†</sup> Université de Montréal.

<sup>‡</sup> Université Laval.

<sup>§</sup> University of Idaho.

\* Corresponding author: Tel (514) 340-5762; Fax (514) 340-5290; e-mail c.pellerin@umontreal.ca.

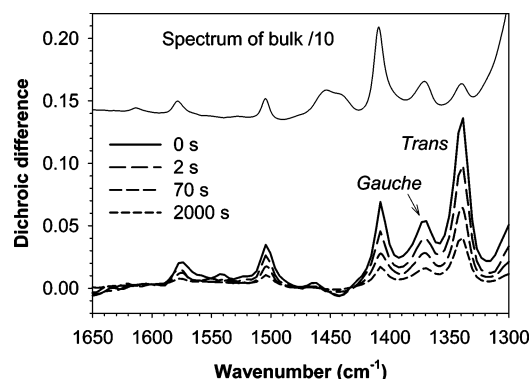


**Figure 1.** (top) Infrared spectrum of an undeformed amorphous PET film and (bottom) dichroic difference spectra recorded immediately (0 s), 2 s, 70 s, and 2000 s following a deformation to a draw ratio of 1.5 at 90 °C.

stretcher fitted with ZnSe windows to allow in-situ recording of the infrared spectra. The draw ratios for the high- and low-temperature experiments were 1.5 and 2.0, respectively, corresponding to deformation times of  $\sim 550$  and  $\sim 900$  ms, respectively. While the deformation above  $T_g$  was homogeneous, the room temperature stretching was highly inhomogeneous and led to a true draw ratio of  $\sim 3.8$  in the necked section of the sample.

PM-IRLD difference spectra with a spectral resolution of  $8\text{ cm}^{-1}$  were acquired using a Bomem Michelson MB-100 FTIR spectrometer equipped with a photovoltaic MCT detector (Kolmar Technologies). The optical setup and the two-channel acquisition electronics required for performing PM-IRLD experiments were described in detail elsewhere.<sup>14</sup> URS-FTIR measurements were performed with a spectral resolution of  $6\text{ cm}^{-1}$ , using the spectrometer designed by Manning Applied Technology.<sup>1,7,12</sup>

The orientation function,  $\langle P_2(\cos \theta) \rangle$ , was calculated from either the dichroic ratio ( $R = A_p/A_s$ ) or the dichroic difference ( $\Delta A = A_p - A_s$ ) for the URS-FTIR and PM-IRLD experiments, respectively, using<sup>2</sup>

$$\langle P_2(\cos \theta) \rangle = \frac{2}{3 \cos^2 \alpha - 1} \frac{R - 1}{R + 2} = \frac{2}{3 \cos^2 \alpha - 1} \frac{\Delta A}{3 A_0} \sqrt{\lambda} \quad (1)$$

where  $A_p$  and  $A_s$  are the absorbances measured with the radiation polarized parallel and perpendicular to the stretching direction, respectively,  $\alpha$  is the angle between the transition moment of the vibration and the main chain axis of the polymer, and  $\lambda$  is the draw ratio. The absorbance of the isotropic sample prior to deformation,  $A_0$ , was determined using a Nicolet Magna 550 FTIR spectrometer. Both this instrument and a Bruker Vertex 70 FTIR spectrometer were used to record static polarized and unpolarized spectra of the samples. For the URS-FTIR experiments, two separate samples were deformed in order to record successively the p and s time-resolved spectra.

## Results and Discussion

### Polarization Modulation Infrared Linear Dichroism.

Figure 1 shows three PM-IRLD spectra, recorded immediately at the end of the deformation (0 s) and after 2 s, 70 s, and 2000 s of relaxation at constant strain, in addition to a standard infrared spectrum of the bulk sample. The baseline of the latter spectrum was raised and the absorbance scale was reduced by a factor 10 for clarity. The bands at  $1340$  and  $1370\text{ cm}^{-1}$  are assigned to the wagging vibrations of the glycol  $\text{CH}_2$  groups in the trans and gauche conformations, respectively, while the  $1410\text{ cm}^{-1}$  band has been assigned to an in-plane deformation of the phenyl ring.<sup>15</sup> A positive dichroism can be observed for all three bands, but their relative intensity in the dichroic spectra is quite different from that in the spectrum of the bulk PET film. A larger relative orientation is found for the band due to the

methylene groups in a trans conformation, while those in the gauche conformation appear much less oriented, in agreement with published results.<sup>10,11,15–17</sup>

In contrast with the  $1340$  and  $1370\text{ cm}^{-1}$  bands, the  $1410\text{ cm}^{-1}$  band has usually been considered to be insensitive to orientation and conformation and has thus often been used as a thickness standard for studies of PET and other polyesters.<sup>17–19</sup> The difference spectra of Figure 1 nevertheless clearly indicate a significant positive dichroism for this band. The orientation function calculated for the  $1410\text{ cm}^{-1}$  band is about 10% of that for the band at  $1340\text{ cm}^{-1}$ . Although this value appears modest, the use of the  $1410\text{ cm}^{-1}$  band as a thickness standard can nevertheless introduce a significant error if the orientation of the sample is not taken into account. For example, in the case of a PET film with  $\langle P_2(\cos \theta) \rangle = 0.9$  for the trans conformers, the thickness would be overestimated by about 5% using an unpolarized spectrum and by as much as 18% for a p-polarized spectrum.

This problem can be overcome by using a structural absorbance spectrum to determine the sample thickness rather than a single polarized or unpolarized spectrum. Calculation of a structural absorbance spectrum requires knowledge of the absorbance along the three principal axes of the sample, which can be obtained by measuring a polarized spectrum at oblique incidence in addition to polarized spectra at normal incidence.<sup>4</sup> If the sample presents uniaxial (fiber) symmetry, the absorbance along the two axes orthogonal to the drawing direction can be assumed to be identical, so that only polarized spectra measured at normal incidence are needed. While this is easily done for static measurements, it should be noted that this procedure is more challenging for time-resolved studies since the dichroic difference is measured directly in a PM-IRLD experiment.

In addition to an increased sensitivity as compared to conventional infrared linear dichroism, PM-IRLD provides a much faster time resolution for dynamic studies. Indeed, the dichroic difference spectra of Figure 1 were recorded from a single scan of 400 ms. This rapid acquisition enables PM-IRLD to follow in real-time the relaxation dynamics of deformed polymers, as was demonstrated for PET<sup>10,20</sup> and other homopolymers,<sup>6,21</sup> for polymer blends,<sup>8,22</sup> and for copolymers.<sup>9</sup> The value of such time resolution is obvious when comparing the spectra recorded at times 0 and 2 s in Figure 1. As much as 40% of the segmental orientation is lost within the first 10 s following the end of the deformation.

Although their absolute orientation values are quite different, the relaxation of orientation for the gauche and trans conformers follows very similar kinetics (not shown), as first observed by Duchesne et al.<sup>10</sup> Since the angle  $\alpha$  is not known for the  $1410\text{ cm}^{-1}$  band, it is not possible to determine the value of  $\langle P_2(\cos \theta) \rangle$  from this band. It is nevertheless possible to compare the relaxation kinetics of the transition dipole associated with this band with that of the trans conformers by normalizing the orientation function to a value of 1 at the end of the deformation process (i.e., at time  $t = 0$  s in the relaxation period). Figure 2 shows that similar curves are obtained for the  $1410$  and  $1340\text{ cm}^{-1}$  bands at short relaxation times. To our knowledge, this is the first time that the relaxation dynamics of the phenyl ring of PET have been observed directly and independently. It can be observed that the relaxation curves begin to diverge for relaxation times longer than 1000 s. The phenomenon appears to be reproducible from sample to sample, but it should be acknowledged that the dichroic difference in this part of the relaxation curve is quite weak, ca. 0.015 AU, which makes the measurement sensitive to systematic errors such as a drift in

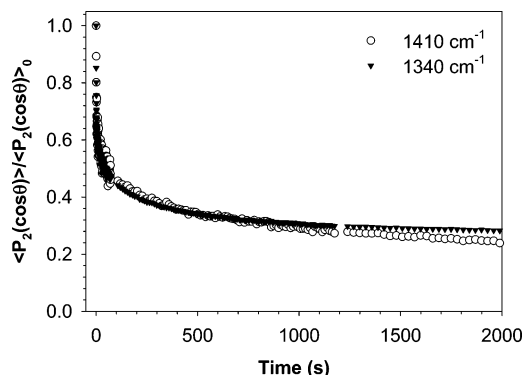


**Figure 2.** Orientation relaxation dynamics of the trans conformers ( $1340\text{ cm}^{-1}$ ) and of the phenyl rings ( $1410\text{ cm}^{-1}$ ) of amorphous PET following a deformation to a draw ratio of 1.5 at  $90\text{ }^{\circ}\text{C}$ .

the baseline. The results of Figure 2 strongly suggest that, at least for the first 1000 s, the phenyl rings of the terephthalate moiety relax with similar kinetics as the methylene groups in amorphous PET.

As noted above, Duchesne et al. have shown that the relaxation of the gauche and trans conformers follow the same kinetics.<sup>10</sup> It has also been noted, in a previous paper, that the  $3336\text{ cm}^{-1}$  band (combination of the carbonyl stretch with the  $\nu_{8b}$  phenyl deformation) and the overtone of the carbonyl stretching vibration ( $3433\text{ cm}^{-1}$ ) both behave as the  $1340\text{ cm}^{-1}$  band.<sup>20</sup> The new results reported are in line with these reports and further justify the agreement observed by Oultache et al. between the relaxation curves obtained using PM-IRLD and time-resolved birefringence.<sup>23</sup> Taken together, these observations suggest that the relaxation of amorphous PET proceeds mainly via a cooperative process involving at least one repeat unit and not solely through rotations around the more flexible  $\text{CH}_2\text{--CH}_2$  and  $\text{CH}_2\text{--O}$  links. To further investigate this hypothesis, studies will be performed on polyesters containing a different number of methylene groups, such as poly(propylene terephthalate) and poly(butylene terephthalate).

**Ultrarapid-Scanning Fourier Transform Infrared Spectroscopy.** We have recently demonstrated that URS-FTIR spectroscopy can be used to follow both the deformation and the early part of the orientation relaxation of stretched polymers with a time resolution of 40 ms, corresponding to an improvement of an order of magnitude over previous orientation measurements using infrared spectroscopy.<sup>11</sup> In this work, URS-FTIR has been used to follow the rapid ( $\sim 2.2\text{ cm/s}$ ) cold-drawing of amorphous PET samples at room temperature, well into the glassy state. Under such conditions, the deformation was highly inhomogeneous and proceeded via neck formation and propagation. Figure 3 shows infrared spectra recorded in 5 ms with p-polarized light before and after the elongation of the sample. Very important differences can be observed between the two spectra. As expected, the  $1410\text{ cm}^{-1}$  band is weaker in the deformed sample because the thickness of the film decreases markedly during stretching and its absorbance in the p-polarized spectra increases only modestly due to its weak orientation. In contrast, the band assigned to the gauche conformers at  $1370\text{ cm}^{-1}$  becomes very weak, while that due to the trans conformers at  $1340\text{ cm}^{-1}$  becomes much more intense as deformation proceeds. Some unexpected shoulders or dips appear in the spectra of Figure 3 around  $1346$ ,  $1360$ , and  $1375\text{ cm}^{-1}$  because of an imperfect background correction of the water vapor bands (the URS-FTIR spectrometer was not purged). These artifacts influence the band areas but only have a small influence on time evolution of the band height considered throughout the rest of this paper.

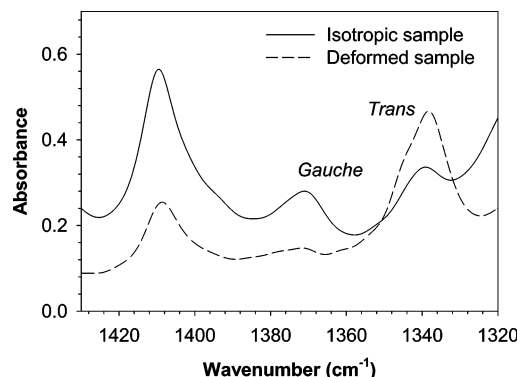


**Figure 3.** p-polarized infrared spectra recorded before and after necking during the room temperature cold drawing of PET. The spectra were recorded with a 5 ms acquisition time.

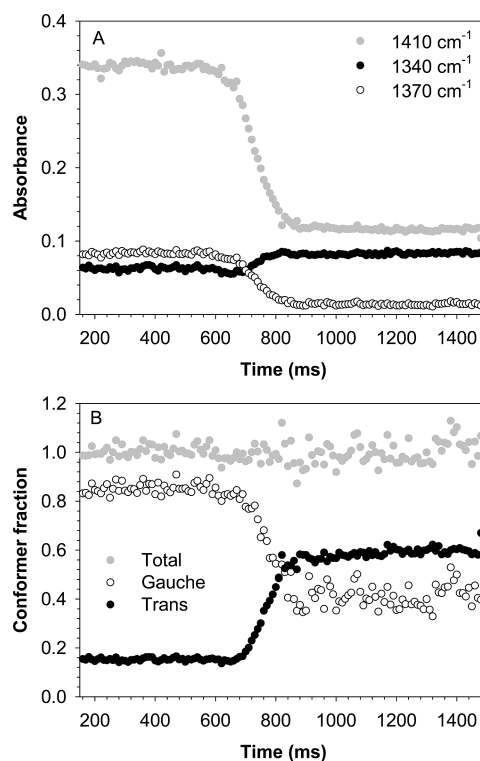


**Figure 4.** Evolution of (A) the structural absorbance of the  $1410$ ,  $1370$ , and  $1340\text{ cm}^{-1}$  bands and (B) the fraction of gauche and trans conformers, for a PET sample deformed at room temperature.

The spectral changes observed in Figure 3 are due to the combined effects of sample thinning, molecular orientation, and conformational changes. To isolate the effect of the conformational changes from that of molecular orientation, the structural absorbance spectra have been calculated as  $A_0 = (A_p + 2A_s)/3$ , assuming uniaxial symmetry. Figure 4A shows the evolution of the structural absorbance for the  $1410$ ,  $1370$ , and  $1340\text{ cm}^{-1}$  bands during drawing with a 10 ms time resolution. It can be observed that the absorbance of all the bands remains constant up to  $\sim 650\text{ ms}$  into the deformation. This does not mean that necking has not formed during this time, as it may be propagating outside the sample section probed by the infrared radiation. However, the result indicates that, in contrast with the homogeneous deformation above  $T_g$ , the sample thickness does not decrease and that no conformational changes are taking place in the sample outside of the neck during the room temperature deformation of PET. During the following 200 ms, the necking front crossed the optical path of the infrared radiation and resulted in an important decrease of the absorbance



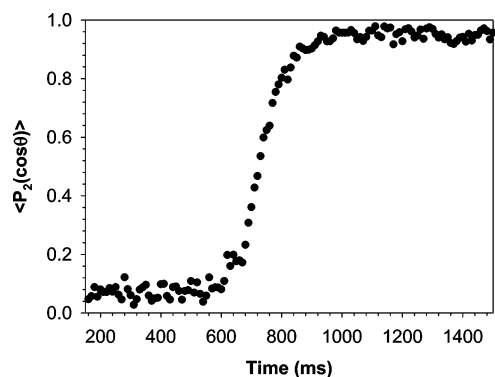


**Figure 5.** Evolution of the orientation function for the trans conformers during the room temperature cold drawing of PET.

of the  $1410\text{ cm}^{-1}$  band because of sample thinning in the neck. This is accompanied by the almost complete loss of the gauche band at  $1370\text{ cm}^{-1}$  and by a significant increase of the trans band at  $1340\text{ cm}^{-1}$ . The absorbance increase for the band attributed to the trans conformers is smaller than the decrease of that for the gauche conformers because both bands are simultaneously affected by sample thinning.

In Figure 4B, the actual fraction of gauche and trans conformers in the sample are plotted as a function of time. These fractions were calculated using the procedure described by Guévremont et al.<sup>16</sup> This procedure requires the use of the  $1410\text{ cm}^{-1}$  band as a standard because the film thickness is different for every spectrum during the deformation, and its evolution during necking is not known a priori. As demonstrated above using PM-IRLD, this band is influenced by the orientation of the sample. However, the use of structural absorbance spectra in the calculations allowed removing the orientation effect (assuming uniaxial symmetry). Figure 4B shows that the film initially contained about 15% of trans conformers, in good agreement with published values for amorphous PET.<sup>15,16,24</sup> Upon necking, the trans-to-gauche ratio changes drastically within a short period of time, with  $\sim 60\%$  of trans conformers present in the fully necked sample. It should be emphasized that the calculated values are not strictly quantitative because (1) it is assumed that the necking formation was identical in two independent deformations performed with p- and s-polarized light and (2) since the necking did not occur at the exact same time for the two deformations, the time axis had to be shifted for the series of spectra.

In addition to the gauche-to-trans conformational changes, necking also introduces molecular orientation in the sample. Figure 5 shows the orientation function calculated using eq 1 for the trans conformers during and following deformation. The angle  $\alpha$  was assumed to be  $18^\circ$  for these calculations.<sup>25</sup> It can be observed in Figure 5 that the original sample was somewhat anisotropic due to the blow-molding process used to prepare the film. When necking crossed the optical path, a very large orientation rapidly developed along the stretching direction. In fact, the orientation function reaches a value of 0.95, very close to the value of 1 that can be expected for a perfectly oriented sample.<sup>4</sup> Conventional IRLD measurements performed after the deformation confirmed quantitatively this orientation function. It can be noted that an angle of  $21^\circ$  has very often been used to calculate the orientation of the  $1340\text{ cm}^{-1}$  band.<sup>10,16–18,20,26</sup> However, this angle yielded values for the orientation function that were larger than unity in this experiment, indicating that  $18^\circ$  is a better approximation.

In contrast with the results obtained for the trans conformers, no significant orientation was discernible for the gauche

conformers by either URS-FTIR or conventional IRLD, while the  $1410\text{ cm}^{-1}$  band showed a positive orientation, as expected from the above, with a dichroic ratio of 1.2. No significant orientation could be measured for either band outside of the necked region.

The orientation function for the trans segments, 0.95, is much higher than that predicted by the affine model of polymer deformation.<sup>2,27</sup> Indeed, considering that the real draw ratio is 3.8 in the necked part of the sample, the affine model predicts a  $\langle P_2(\cos \theta) \rangle$  value of around 0.2. Since this model was designed to describe the orientation of elastomers in the rubbery state, it is not very surprising to find such discrepancy in the case of the cold drawing of PET, which is in the glassy state at room temperature. The pseudo-affine deformation model,<sup>2</sup> which often yields better predictions for semicrystalline or glassy polymers, predicts a  $\langle P_2(\cos \theta) \rangle$  value of 0.73, still below the experimental result. However, it may be more relevant to compare the overall orientation in the sample, as would be observed using birefringence rather than the sole orientation of the trans conformers. Considering that 40% of the sample exists as unoriented gauche conformers (see Figure 4B), we can estimate the overall orientation function to 0.57, well within the limiting cases of the affine and pseudo-affine models.

The results of Figures 4 and 5 clearly show a gauche-to-trans rearrangement and the development of a very large orientation upon stretching of amorphous PET at room temperature. Both appear to be irreversible, since the intensity of the bands in Figure 4A, the conformer fractions in Figure 4B, and the orientation function in Figure 5 remain more or less constant following the end of the deformation, in sharp contrast with the relaxation of orientation observed when deformation is performed above  $T_g$  (Figure 2). Actually, no orientation relaxation could be observed even several months after the initial experiment. At first sight, these different observations could be pointing toward a stress-induced crystallization of the sample. Indeed, postdeformation measurements have shown that the effective draw ratio in the necked region is about 3.8, in agreement with reports indicating that stress-induced crystallization of PET occurs above a draw ratio of 2.5 when it is deformed above  $T_g$ .<sup>17,18,28</sup> Nevertheless, close inspection of the infrared data reveals significant differences between the spectrum of this cold-drawn PET film and that of a heat-crystallized sample.

Cole et al. have used principal components analysis (PCA) to reveal the existence of three contributing structures in the infrared spectra of PET, the so-called G, TX, and TC arrangements.<sup>15,25</sup> The G structure was ascribed to the gauche conformation of the glycol group and disordered terephthalate groups. In contrast, the TX and TC arrangements would both be due to long sequences of repeat units possessing a trans conformation of the glycol group, with disordered and ordered terephthalate groups, respectively. In the TC structure, the PET chains are in a linear, planar, all-trans conformation that favors crystalline packing. The G, TC, and TX structures have important contributions in the amorphous, the crystalline, and the so-called "mesomorphic" (also referred to as "oriented amorphous") phases of PET, respectively.<sup>15,25</sup>

Figure 6 compares the spectra recorded for the undeformed and necked portions of the drawn sample with those extracted from PCA analysis for the G, TX, and TC structures. In both the high- and low-frequency regions, clear spectral differences (changes in band position and width) can be observed between the G, TX, and TC spectra. As expected, the crystalline TC spectrum possesses narrower bands. Qualitative comparison reveals that the experimental spectrum obtained for the unde-

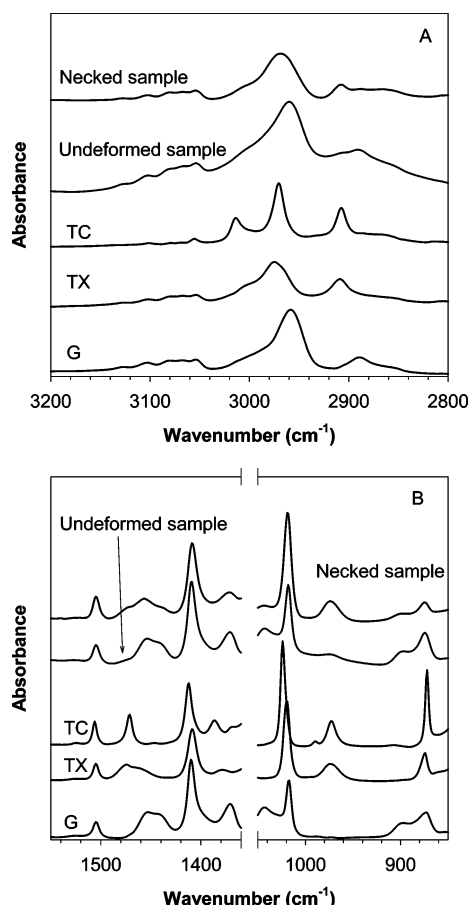


**Figure 6.** Comparison of the experimental infrared spectra, recorded for the necked and undeformed parts of a cold-drawn PET sample, with the G, TX, and TC basis spectra obtained from principal components analysis<sup>15,25</sup> in the high (A) and low (B) frequency regions. The spectra have been scaled for clarity.

formed part of the sample is a good match, although not perfect, with the G spectrum. A curve fitting was performed using the three basis spectra, G, TX, and TC, provided by Cole et al.<sup>15,25</sup> Although it should be considered as semiquantitative at best, this analysis reveals that the undeformed portion of the sample contained  $\sim 80\%$  and  $\sim 20\%$  of the G and TX structures, respectively. This result indicates that this part of the sample remained amorphous during the cold drawing. Indeed, these values are in fair agreement with conformer fractions reported in the literature as well as with the results of Figure 4B for the initial sample. On the other hand, the spectrum of the necked portion of the sample shows, for instance, a large increase of the bands at 970 and 2905  $\text{cm}^{-1}$  as well as several band shifts. Semiquantitative analysis shows that these changes are due to the formation of a large amount,  $\sim 60\%$ , of the TX structure. In contrast, almost no TC is present in the sample. This result is also in excellent agreement with those of Figure 4B after the end of the deformation. Raman spectra (not shown) of the necked section of the sample also show that the carbonyl band possesses a full width at half-height of 27  $\text{cm}^{-1}$  as compared to 16  $\text{cm}^{-1}$  for a heat-crystallized sample. This further suggests that the trans conformers formed during cold drawing are present in the mesomorphic phase (TX) and not in the all-trans (TC) crystalline structure.<sup>29</sup> It is thus interesting to realize that the long-term stability of the large molecular orientation and of the conformer population not only is characteristic of the all-trans crystalline phase but also is observed in the case of the deformation-induced mesomorphic phase of PET.

## Conclusion

Polarization modulation infrared linear dichroism (PM-IRLD) and ultrarapid-scanning Fourier transform infrared (URS-FTIR) spectroscopy have been used to follow the orientation development and conformational changes during the deformation and relaxation of orientation of amorphous PET. PM-IRLD has allowed following the orientation relaxation of the gauche and trans conformers with a 400 ms time resolution. Results have revealed that the 1410  $\text{cm}^{-1}$  band due to the phenyl rings of PET does show a significant dichroism, which relaxes with similar kinetics as that of the glycol segments. The recently developed URS-FTIR technique has allowed the deformation of a cold-drawn amorphous PET sample to be followed with a 10 ms time resolution. Results have shown that necking of the sample generates a large conversion of the gauche segments to the trans conformation and that these trans conformers develop a very large and stable orientation. Spectral analysis suggests that the amorphous sample is converted into the mesomorphic and not into the truly crystalline phase.

A fundamental difference between PM-IRLD and URS-FTIR is that the former technique measures the dichroic difference directly, while the latter technique can only measure spectra with a single polarization at a time. For this reason, PM-IRLD is more sensitive to low dichroism and is less affected by sample variations and instrumental drifts than conventional IRLD and URS-FTIR measurements. It is thus the tool of choice for studies of molecular orientation when its time resolution is sufficient. In contrast, URS-FTIR possesses a much better time resolution that could, in principle, attain 1 ms per spectrum. It is also more flexible, allowing, for instance, conformational changes to be followed in real time. The two techniques can thus be used as complementary tools in the study of polymer deformations.

**Acknowledgment.** This work was supported by NSERC of Canada, FQRNT of the Province of Québec, and NSF. The authors are greatly indebted to Dr. Kenneth C. Cole of the Industrial Materials Institute of the National Research Council of Canada for the generous gift of the PET samples, for providing the reference spectra, and for useful discussions.

## References and Notes

- (1) Yang, H.; Griffiths, P. R.; Manning, C. J. *Appl. Spectrosc.* **2002**, *56*, 1281.
- (2) Ward, I. M., Ed. *Structure and Properties of Oriented Polymers*, 2nd ed.; Chapman & Hall: London, 1997.
- (3) Kalkar, A. K.; Siesler, H. W.; Zebger, I.; Pfeifer, F.; Ameri, A.; Michel, S.; Hoffmann, U. Rheo-optical Fourier Transform Infrared Spectroscopy of Polymers. In *Handbook of Vibrational Spectroscopy*; Griffiths, P. R., Chalmers, J. M., Eds.; John Wiley & Sons: Chichester, 2001; Vol. 1, p 2559.
- (4) Buffeteau, T.; Pérolet, M. Linear Dichroism in Infrared Spectroscopy. In *Handbook of Vibrational Spectroscopy*; Griffiths, P. R., Chalmers, J. M., Eds.; John Wiley & Sons: Chichester, 2001; Vol. 1, p 693.
- (5) Aiji, A.; Zhang, X.; Elkoun, S. *Polymer* **2005**, *46*, 3838. Faivre, J. P.; Jasse, B.; Monnerie, L. *Polymer* **1985**, *26*, 879. Tassin, J. F.; Baschwitz, A.; Moise, J.-Y.; Monnerie, L. *Macromolecules* **1990**, *23*, 1879.
- (6) Buffeteau, T.; Desbat, B.; Pérolet, M.; Turlet, J. M. *J. Chim. Phys. Phys.-Chim. Biol.* **1993**, *90*, 1467.
- (7) Griffiths, P. R.; Hirsche, B. L.; Manning, C. J. *Vib. Spectrosc.* **1999**, *19*, 165.
- (8) Pellerin, C.; Prud'homme, R. E.; Pérolet, M. *Macromolecules* **2000**, *33*, 7009.
- (9) Wang, Y. X.; Pellerin, C.; Bazuin, C. G.; Pérolet, M. *Macromolecules* **2005**, *38*, 4377.
- (10) Duchesne, C.; Kong, X. H.; Brisson, J.; Pérolet, M.; Prud'homme, R. E. *Macromolecules* **2002**, *35*, 8768.
- (11) Pellerin, C.; Prud'homme, R. E.; Pérolet, M.; Weinstock, B. A.; Griffiths, P. R. *Macromolecules* **2003**, *36*, 4838.

- (12) Manning, C. J. Spectrometer for spectroscopic measurement in infrared spectral region, spectral imaging. US Pat. 5 898 495, 27 Apr 1999.
- (13) Weinstock, B. A.; Yang, H. S.; Griffiths, P. R. *Vib. Spectrosc.* **2004**, 35, 145. Weinstock, B. A.; Yang, H. S.; Hirsche, B. L.; Griffiths, P. R. *Langmuir* **2005**, 21, 3915.
- (14) Pézolet, M.; Pellerin, C.; Prud'homme, R. E.; Buffeteau, T. *Vib. Spectrosc.* **1998**, 18, 103.
- (15) Cole, K. C.; Ajji, A.; Pellerin, E. *Macromolecules* **2002**, 35, 770.
- (16) Guèvremont, J.; Ajji, A.; Cole, K. C.; Dumoulin, M. M. *Polymer* **1995**, 36, 3385.
- (17) Lu, X. F.; Hay, J. N. *Polymer* **2001**, 42, 8055.
- (18) Matthews, R. G.; Ajji, A.; Dumoulin, M. M.; Prud'homme, R. E. *Polymer* **2000**, 41, 7139.
- (19) Park, S. C.; Liang, Y.; Lee, H. S. *Macromolecules* **2004**, 37, 5607.
- (20) Pellerin, C.; Rousseau, M. E.; Prud'homme, R. E.; Pézolet, M. *Appl. Spectrosc.* **2002**, 56, 17.
- (21) Messé, L.; Pézolet, M.; Prud'homme, R. E. *Polymer* **2001**, 42, 563.
- (22) Pellerin, C.; Pelletier, I.; Pézolet, M.; Prud'homme, R. E. *Macromolecules* **2003**, 36, 153. Messé, L.; Prud'homme, R. E. *J. Polym. Sci., Part B: Polym. Phys.* **2000**, 38, 1405.
- (23) Oultache, A. K.; Kong, X.; Pellerin, C.; Brisson, J.; Pézolet, M.; Prud'homme, R. E. *Polymer* **2001**, 42, 9051.
- (24) Rodriguez-Cabello, J. C.; Quintanilla, L.; Pastor, J. M. *J. Raman Spectrosc.* **1994**, 25, 335.
- (25) Cole, K. C.; Ajji, A.; Pellerin, E. *Macromol. Symp.* **2002**, 184, 1.
- (26) Cole, K. C.; Guèvremont, J.; Ajji, A.; Dumoulin, M. M. *Appl. Spectrosc.* **1994**, 48, 1513. Spiby, P.; O'Neill, M. A.; Duckett, R. A.; Ward, I. M. *Polymer* **1992**, 33, 4479.
- (27) Roe, R. J.; Krigbaum, W. R. *J. Appl. Phys.* **1964**, 35, 2215.
- (28) Ajji, A.; Guèvremont, J.; Cole, K. C.; Dumoulin, M. M. *Polymer* **1996**, 37, 3707. Middleton, A. C.; Duckett, R. A.; Ward, I. M.; Mahendrasingam, A.; Martin, C. J. *J. Appl. Polym. Sci.* **2001**, 79, 1825.
- (29) Adar, F.; Noether, H. *Polymer* **1985**, 26, 1935.

MA0610459